CHEMISTRY
A European Journal

A Journal of
ChemPubSoc Europe

Accepted Article

Title: Bistetrazine-cyanines as double-clicking fluorogenic two-point binder or crosslinker probes

Authors: Attila Kormos, Christine Koehler, Eszter Fodor, Zsófia Rutkai, Maddison Martin, Gábor Mező, Edward Lemke, and Péter Kele

To be cited as: *Chem. Eur. J.* 10.1002/chem.201800910

Link to VoR: http://dx.doi.org/10.1002/chem.201800910

Supported by
ACES

WILEY-VCH

10.1002/chem.201800910

WILEY-VCH

FULL PAPER

Bistetrazine-cyanines as double-clicking fluorogenic two-point binder or crosslinker probes

Attila Kormos,[a] Christine Koehler,[b,c,d] Eszter A. Fodor,[a] Zsófia R. Rutkai,[a] Madison E. Martin,[a] Gábor Mező,[e] Edward A. Lemke,*[b,c,d] and Péter Kele*[a]

Abstract: Fluorogenic probes are capable of minimizing background fluorescence of unreacted and non-specifically adsorbed reagents. The preceding years have brought substantial developments in the design and synthesis of bioorthogonally applicable fluorogenic systems mainly based on the quenching effects of azide and tetrazine moieties. The modulation power exerted by these bioorthogonal motifs typically becomes less efficient on more conjugated systems, i.e. on probes with red-shifted emission wavelength. In order to reach efficient quenching, i.e. fluorogenicity even in the red range of the spectrum, We present the synthesis, fluorogenic and conjugation characterization of bistetrazine-cyanine probes with emission maxima between 600–620 nm. The probes can bind to genetically altered proteins harboring an 11-amino acid peptide tag with two appending cyclooctyne motifs. Moreover, we also demonstrate the use of these bistetrazines as fluorogenic, covalent cross-linkers between monocyclooctynylated proteins.

Introduction

Exploration of intra- or extracellular processes through fluorescent imaging of biomolecules showed great advancements in the last decade.[1–6] These improvements were greatly facilitated by the development of probes capable of (site)specific tagging of biomolecules of interest. Although fluorescent modulation of a wide range of biomolecules e.g. proteins, nucleic acids, lipids, sugars, small metabolites etc. is possible, specific labeling of proteins is still the major focus for cell biological studies. Several techniques are used to address these tasks e.g. the use of fusion proteins such as tailored fluorescent proteins (FPs), tags (e.g. Halo, SNAP, Cys_4) or small engineered enzymes (e.g. lipoic acid ligase).[1–6] In some cases these fusion tags may alter the original function of the protein of interest (POI) due to their comparable size. Advances in genetic code expansion (GCE) methods by means of Amber codon suppression in combination with bioorthogonal chemistry have opened a new horizon in the field of site-specific tagging schemes enabling single amino acid incorporation virtually at any positions of the POI with minimal perturbation.[7–10] In such labeling schemes genetic incorporation of a bioorthogonalized, noncanonical amino acid (ncAA) is followed by a specific reaction with a small synthetically tailored dye. Limitations of imaging techniques that rely on small synthetic probes are often associated with autofluorescence and/or background fluorescence.[11] While the former is readily suppressed by dyes that are either excitable towards the red range of the spectrum or possess large Stokes-shifts, background fluorescence of non-specifically adsorbed probes is efficiently reduced by using fluorogenic probes. Since the unreacted forms of fluorogenic probes obey quenched fluorescence, minimal, ideally zero non-specific signal originates from these species.[12]

It can be considered a fortunate coincidence that upon careful design, certain bioorthogonally applicable functional groups such as the azide and the tetrazine are capable of quenching the fluorescence of signaling frames. The two-in-one feature of these chemical functions was harvested in the design and synthesis of a series of bioorthogonally applicable fluorogenic probes.[13–16] There are several explanations in the literature for the quenching mechanism present in these systems. To name a few, photoinduced electron transfer (PET)[13], through-bond energy transfer (TBET)[15] , Förster resonance energy transfer (FRET)[6,16] or in case of azides, increased efficiency of internal conversion as a result of fast rotation and bending of the azide[14] (for detailed discussion of possible quenching mechanisms see Ref. 17). For tetrazine quenched systems, where the fluorescent frame is linked to the tetrazine through conjugated but electronically decoupled spacers TBET is widely accepted, however, PET-based quenching is also viable. Regardless of the exact mechanism, tetrazines are quite efficient quencher moieties especially in cases when the fluorophore has small, compact structure. It can be noted, however, that the quenching effect exerted by either an azide or a tetrazine is less efficient in case of scaffolds with more extended conjugation. As a consequence, the fluorescence increase upon conjugation to targets (i.e. fluorogenicity) decreases.[13–15] We believe that probes that

[a] Dr. A. Kormos, Ms. E. A. Fodor, Ms. Zs. R. Rutkai, Ms. M. E. Martin, Dr. P. Kele
Institute of Organic Chemistry, Research Centre for Natural Sciences, Hungarian Academy of Sciences
H-1117, Budapest, Magyar tudósok krt. 2. Hungary
E-mail: kele.peter@ttk.mta.hu
[b] Dr. C. Koehler, Prof. Dr. E. A. Lemke
Departments of Biology and Chemistry, Pharmacy and Geosciences, Johannes Gutenberg-University Mainz, Johannes-von-Mullerweg 6, 55128 Mainz, Germany.
[c] Institute of Molecular Biology (IMB), Ackermannweg 4, 55128 Mainz, Germany.
[d] EMBL, Meyerhofstrasse 1, 69117 Heidelberg Germany. e-mail: edlemke@uni-mainz.de
[e] Prof. G. Mező
MTA-ELTE Research Group of Peptide Chemistry, Hungarian Academy of Sciences, Pázmány Péter sétány 1a, H-1117, Budapest, Hungary

Supporting information for this article is given via a link at the end of the document. (Details of synthetic procedures, characterization data for small molecules, fluorescence spectra, kinetic experiments, peptide and protein labeling experiments are provided.)

possess extremely high fluorogenicity (e.g. coumarin-based HELIOS probes)[15b] are predominantly quenched by the tetrazine, thus a more profound fluorogenic effect is observed upon reaction. In case of red-shifted systems with more extended conjugation, other non-radiative mechanisms such as vibrational relaxation, internal conversion etc. become more dominant and less effect is exerted by the tetrazine. Thus, we speculate that the lower fluorogenicity observed for red-shifted systems is due to the less dominant role of the quencher moiety. Relying on literature examples for two-point binder fluorogenic probes, such as biarsenicals[18] or bismaleimides[19], we set forth investigating the possibility of multiple quenching by biorthogonal motifs. Recently, we designed a set of bisazide probes and verified our hypothesis against a series of biscyclooctynylated peptide scaffolds.[20] Thorough studies involving mono-quenched congeners facilitated the assessment of the contribution of the individual quencher motifs to the overall fluorogenicity.[20] The concept was successfully extended and applied to biologically more favorable fluorescent cores (e.g. cyanines) addressing the problem arising from the reverse relationship between fluorogenicity and extended conjugation (i.e. quenching becomes less efficient towards the red end of the spectrum).[20b] We also aimed at demonstrating that such bisazide fluorogens are useful probes in the labeling schemes of genetically double-cyclooctynylated model proteins.[20b] High yielding expression of double-Amber suppressed proteins is more difficult than single Amber suppression though efforts into this direction continuously improve yields.[21–23] Moreover, the reported bisazides were prone to daylight degradation and thus required particularly careful handling.[20,24] These observations prompted us to design and construct bis-quenched probes with more reactive biorthogonal handles and designed bistetrazine fluorogenic scaffolds. As fluorescent cores we kept the cyanine frame due to the advantageous features of this dye family that make them prime choices in fluorescence microscopy applications e.g. suitable photostability, large absorption cross-sections, compatibility with common lasers and super-resolution techniques.[25,26] Furthermore, we also aimed to demonstrate the use of these bistetrazine scaffolds as fluorogenic crosslinking platforms to covalently link mono-cyclooctynylated proteins.

Results and Discussion

Synthesis of bistetrazine probes

The synthesis started with hydrazination of *p*-iodoaniline (**1**) via treatment with $NaNO_2$ and subsequent reduction using $SnCl_2{\cdot}2H_2O$. Hydrazine **2** was then refluxed in AcOH in the presence of 3-methyl-2-butanone to provide iodoindole **3** that was treated with EtI to access indolium salt **4** in medium yield. The cyanine frame, **5**, was formed by allowing **4** to react with triethylorthoformate in pyridine under reflux. Diiodocyanine, **5** was then subjected either to Suzuki cross coupling reaction with pinacol 4-(6-methyltetrazin-3-yl)phenylboronate to provide target compound **6** or Heck-type of cross coupling with 2-(6-methyltetrazin-3-yl)ethyl methanesulfonate to result in target compound **7** in fair to medium yields (Scheme 1).

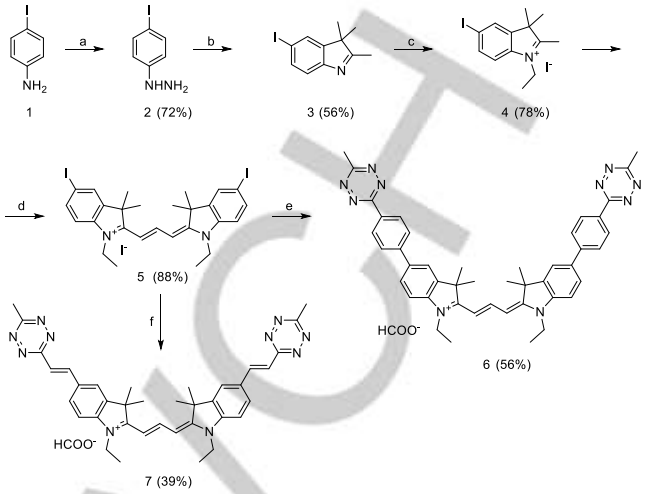

Scheme 1. Synthesis of bistetrazine-cyanines, **6** and **7** (a) 1. $NaNO_2$, 20% HCl, 0°C, 0.5h, 2. $SnCl_2.2H_2O$, concd. HCl, 0°C, 0.5h (b) 3-methyl-2-butanone, AcOH, reflux, 3h (c) EtI, MeCN, reflux, overnight (d) $(EtO)_3CH$, pyridine, reflux, 4h (e) pinacol 4-(6-methyltetrazin-3-yl)phenylboronate, $Pd(dppf)Cl_2$, CsF, MeCN, reflux, overnight (f) 2-(6-methyltetrazin-3-yl)ethyl methanesulfonate, Pd_2dba_3, QPhos, Cy_2NMe, DMF, 100°C MW, 1h.

Table 1. Photophysical properties and fluorogenicity of dyes **6** and **7** and their conjugates[a]

			bistetrazine		+BCN			+ peptide		
	[b]λ_{exc} (nm)	[b]λ_{em} (nm)	[c]ε	[d]Φ_0	[c]ε	[d]Φ	Φ/Φ_0	[c]ε	[d]Φ	Φ/Φ_0
6	585 (582)	609 (603)	11.3	2.18	11.1	0.289	13.3	10.6	22.4	10.3
7	605 (599)	624 (619)	10.4	1.14	9.3	0.157	14.8	9.0	11.3	10.0

[a] all reactions and measurements were performed in sodium PBS buffer (pH = 7.4) containing 0.1% SDS with dye concentrations between 1–5 μM. [b] wavelengths in parentheses belong to the conjugates. [c] Calculated at excitation maxima ($\times 10^4$ $M^{-1}cm^{-1}$); [d] Φ values are determined relative to Rhodamine B at λ_{exc} = 510 nm ($\times 10^{-2}$)

Fluorogenicity and kinetic studies

Following the synthetic work we determined the main photophysical properties and fluorogenicity of the new probes upon inverse electron demand Diels–Alder (IEDDA) reaction with a commercially available cyclooctyne (bicyclo[6.1.0]non-4-yn-9-ylmethanol, BCN)[27] and an eleven amino acid peptide sequence developed in our preceding account,[20b] containing terminal Lys residues with appending BCN units at their ε-amino group, Ac-K(BCN)AEAADAEAAK(BCN)-NH_2. To our delight, both probes showed significantly red-shifted excitation and emission maxima in comparison to their respective bisazide congeners[20b] making these new probes better matched to red-channels of fluorescent microscopes.

10.1002/chem.201800910

FULL PAPER

We also measured emission spectra of probes **6** and **7** in solvents with different polarity (e.g. toluene and acetonitrile, see Figure S1 in SI). Emission spectra showed a clear blue-shift in more polar solvent which can be explained by the formation of less polar species in the excited state compared to the ground state with a positive charge present. Only slight differences in intensity of emission was observed in toluene and acetonitrile, suggesting that energy transfer (i.e. TBET) is the dominant mechanism of quenching as redox based quenching (i.e. PET) would have resulted in much lower emission intensity in polar media.[15b, 28]

The probes showed a small blue shift in their excitation and emission maxima upon reaction with 2 equivalents of BCN or 1 equivalent of the peptide. LC-MS measurements affirmed the formation of single products with m/z values corresponding to the cyclic peptide–dye conjugates.

To our pleasure, 10–14 fold fluorescence enhancements were observed upon conjugation (Table 1). The slightly lower fluorescence enhancements in case of the peptide-conjugates can be explained by the out of plane torsion of the conjugated system upon formation of the cyclic products, as discussed in our earlier paper (Figure 1).[20a]

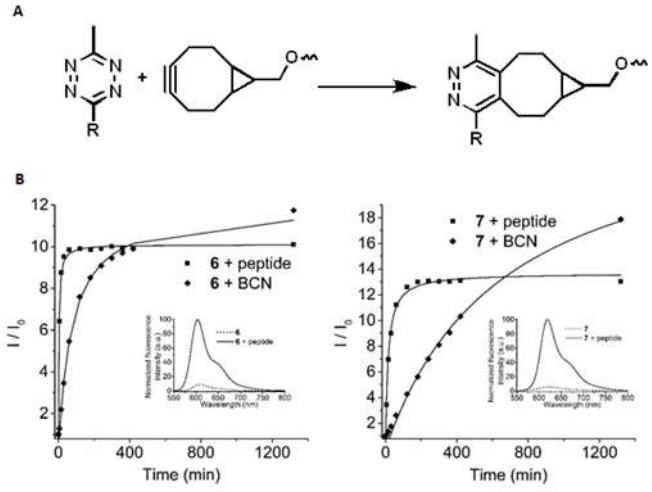

Figure 1. A) Schematic representation of the IEDDA reaction between a tetrazine and BCN; B) Increase in emission of dye **6** (left) and dye **7** (right) when reacted with two equivalents of BCN or one equivalent of peptide (in PBS-SDS pH = 7.4, c = 1 µM, at room temperature).

Reaction of these bisfunctionalized probes is complex and involves either two consecutive intermolecular steps (with BCN) or an intermolecular reaction with a subsequent intramolecular cyclization (with peptide). Therefore we used the method suggested by Keillor *et a*l. for bismaleimides where these reactions are approximated by second order kinetics.[29] This approach relies on the fact that the first, intermolecular step is the rate determining and the second step, regardless of being intra or intermolecular, is much faster. This is supported by the experimental observation that we were unable to isolate mono-reacted species and even with 0.5 equivalent BCN the double-reacted product was observed. Therefore we applied second order conditions in the case of reaction with the peptide and pseudo first-order conditions with BCN (for detailed description see SI and Table S1, Figures S2, S3). Second order rate constants turned out to be somewhat lower than that obtained for bismaleimides[29a] and are in good accordance with literature values measured for methyl-tetrazines.[6] Probe **6** reacted ca. 4 times faster than **7** ($k_2 = 2.6\times10^3$ vs. 6×10^2 $M^{-1}s^{-1}$) with the peptide. The lower k_2 values determined for both probes with BCN ($k_2 = 3.1\times10^2$ for **6** and 1.6×10^2 $M^{-1}s^{-1}$ for **7**, respectively) suggest the importance of an entropy effect in case of the reaction with the peptide.

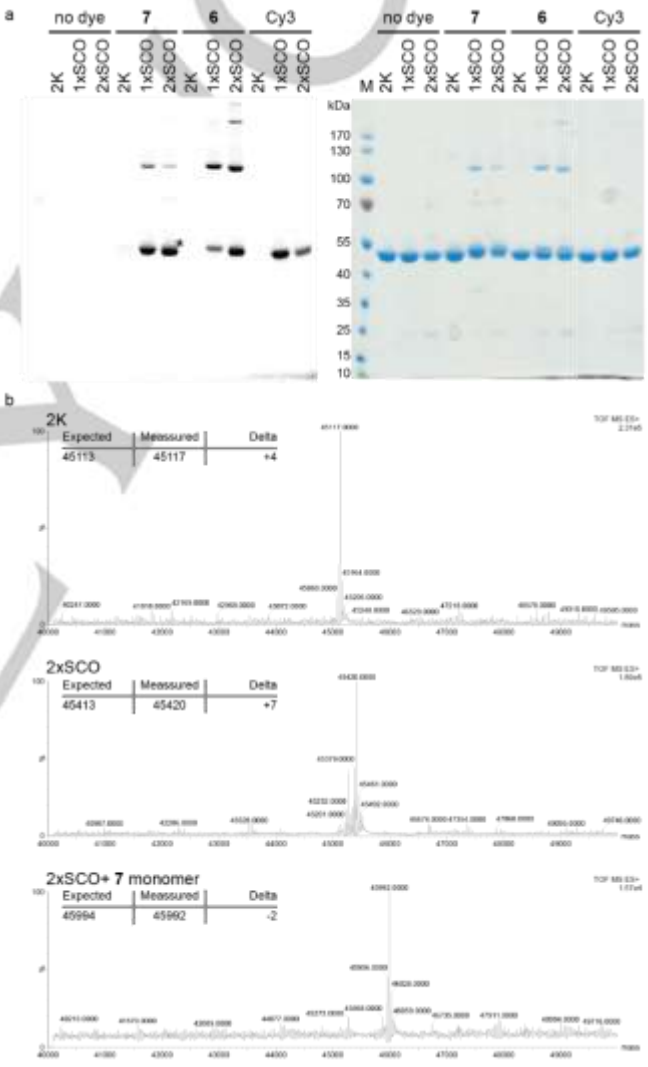

Figure 2. Tagging experiments of MBP construct containing a double-SCO tag at its N-terminus. a) Fluorescent (left) and corresponding Coomassie stained SDS-PAGE (right) of the MBP constructs reacted with probe **6**, **7** and commercially available 6-Methyl-Tetrazine-Cy3 as well as no dyes as controls. The constructs used were 2K = FLAG-K-AEAADAEAA-K-MBP-8His (containing no ncAA), 1xSCO = FLAG-K-AEAADAEAA-SCO-MBP-8His (containing one SCO) and 2xSCO = FLAG-SCO-AEAADAEAA-SCO-MBP-8His (containing two SCO). The asterisk (*) indicates the monomeric labeled 2xSCO-MBP construct. b) Mass spectrometry analysis of the 2K- and 2xSCO-MBP constructs, as well as the 2xSCO-MBP construct labeled with probe **7**. Expected, measured masses and the resulting delta values (in Da) are also shown in the graph.

10.1002/chem.201800910

Protein tagging experiments and cross-linking studies

To explore the applicability of the bistetrazine probes in protein tagging experiments we have designed a maltose-binding protein (MBP) construct modified with a FLAG-tag followed by a double-Amber suppression tag at its N-terminus (FLAG-Amber-AEAADAEAA-Amber-MBP-8His). For the incorporation of a cyclooctyne-lysine, K(SCO), at the Amber sites, we co-expressed the MBP construct in the presence of the *Methanosarcina mazei* pyrrolysine aminoacyl-tRNA-synthetase/tRNA pair ($PylRS^{AF}/tRNA^{Pyl}$, AF indicating a mutated version of PylRS: Y306A and Y384F), in Bl21(DE3) AI cells (Invitrogen) and 1 mM K(SCO) supplied to the growth medium.[7b]

Control constructs, containing a single Amber site (FLAG-K-AEAADAEAA-Amber-MBP-8His) or no Amber site at all (FLAG-K-AEAADAEAA-K-MBP-8His) were prepared as well. The purified proteins were treated with 1 equiv. of dyes **6**, **7** and 6-Methyl-Tetrazine-Cy3 and analyzed by SDS-PAGE (Figure 2a). For the constructs harboring one SCO (FLAG-K-AEAADAEAA-K(SCO)-MBP-8His) and two SCOs (FLAG-K(SCO)-AEAADAEAA-K(SCO)-MBP-8His) fluorescent bands appeared at the size of the MBP indicating successful labeling. Fluorescent bands at double of the size of MBP indicated that some crosslinked species were also formed. In control labeling experiments with monofunctional 6-Methyl-Tetrazine Cy3, only the labeled monomeric species was formed. Control construct without any SCO (FLAG-K-AEAADAEAA-K-MBP-8His) was not labeled at all.

To validate the formation of a cyclic product, the construct containing two SCO residues was labeled with bistetrazine dye **7**, and mass spectrometry analysis was performed (Figure 2b). To retrieve the labeled monomeric species, the construct FLAG-K(SCO)-AEAADAEAA-K(SCO)-MBP-8His labeled with bistetrazine probe **7** was purified by size exclusion chromatography. Mass spectrometry analyses was done for three protein samples (2K, 2×SCO and 2×SCO+**7**, Figure 2b). All delta values (i.e. expected to measured mass value) were within reasonable range taking the size of the protein into account. These results are in line with the formation of a cyclic product when dye **7** is bound at two points to the Flag-K(SCO)-AEAADAEAA-K(SCO)-MBP-8His construct.

To further demonstrate the versatility of our probes, we next investigated their potential as fluorogenic crosslinker platforms. To this end, we expressed GFP-6His containing a single TAG (Amber mutation) at position 39 ($GFP^{Y39\rightarrow TAG}$) by co-expression with the $PylRS^{AF}/tRNA^{Pyl}$ pair and addition of bicyclo[6.1.0]nonyne-lysine, K(BCN) into the growth medium, which resulted in the expression of $GFP^{Y39\rightarrow BCN}$.

In a time-course experiment we reacted $GFP^{Y39\rightarrow BCN}$ with 1 equiv. of bis-tetrazines **6** and **7** and commercially available 6-Methyl-Tetrazine Cy3 as a mono-tetrazine control (Fig. 3). Both bistetrazine probes showed cross-linking behavior already after a few minutes as indicated by the explicit transition of the monomeric species to dimers. In contrast, the mono-tetrazine Cy3-dye only yielded the monomeric labeled $GFP^{Y39\rightarrow BCN}$.

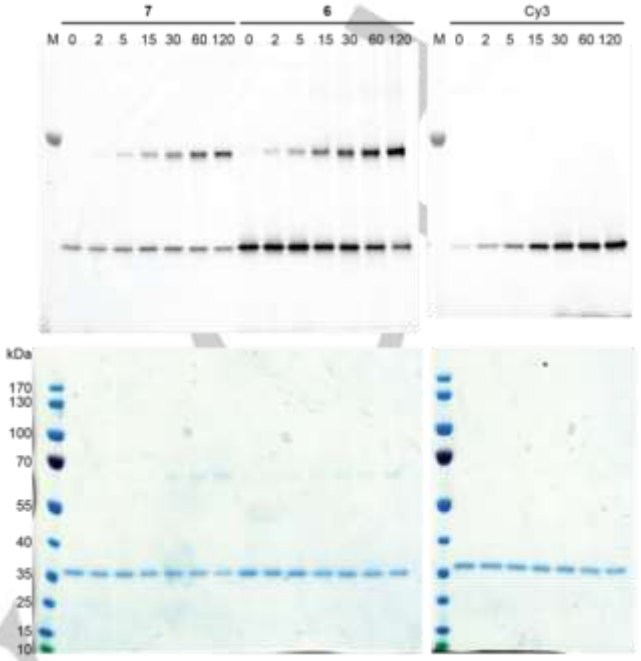

Figure 3. Cross-linking studies of $GFP^{Y39\rightarrow BCN}$ reacting with the bistetrazine probes **6**, **7** and mono-tetrazine Cy3. Fluorescent (top) and corresponding Coomassie stained SDS-PAGE (bottom) of $GFP^{Y39\rightarrow BCN}$ at different time points (in minutes).

Conclusions

Prompted by the challenge that drove us to design red-shifted fluorogenic probes with appreciable fluorogenicity, we applied the concept of multiple quenching by installing two reactive quencher moieties onto fluorescent frames. Such fluorogenic, bis-quenched two-point binders and cross-linkers exist in the literature e.g biarsenicals[30-36], bisboronic[37] acids or bismaleimide[19,29] probes that can be used in tagging schemes in combination with fusion tags involving natural amino acids in a non-natural arrangement (e.g. Cys_4 or Ser_4). These probes are well credited, however, some of them are toxic, they react reversibly, may cross-react with excessive amount of natural thiols and require the presence of free sulfhydryls. Therefore we sought for functions that enable highly selective tagging, use non-toxic chemistry, proceed with reasonable rates at nearly quantitative yields and render fluorescent cores fluorogenic. Formerly, we used two azide groups as bioorthogonally applicable quencher moieties, however, the reaction of azides with cyclooctynes were found to be very slow. This problem was addressed herein by the synthesis of two new bistetrazine, double-quenched, bioorthogonally applicable fluorogenic cyanine probes with emission maxima between 600–620 nm and excitation wavelengths matching well with sources of fluorescent microscopes. We have studied the fluorogenic potential of the probes upon reaction with a biscyclooctynylated peptide and observed 10-fold enhancements in fluorescence. This increase is considered quite remarkable among fluorogenic Cy3 dyes (*cf*. 1.5 – 5 fold increase for AsCy3 biarsenicals)[30,31] and

might be sufficient to allow application in live cell imaging . Unlike bisazide cyanine probes reported in our preceding accounts,[20] these bistetrazines were not that easily prone to degradation by daylight. We explored the labeling potential of these probes on a double-tagged protein, where two bioorthogonalized ncAAs were implemented via Amber suppression technology. Experiments indicated formation of the right cyclic probe–protein conjugate. Since, Amber-tagging with bioorthogonalized ncAAs is not restricted to *N*- or *C*-terminal modifications, these platforms enable mutations virtually at any optimized location. Thus, we envision that this concept, upon further optimization, enables the exploration of enzyme activation/inactivation, conformational changes using minimally perturbed engineered proteins etc.

We also studied the cross-linking potential of these fluorogenic, bifunctional platforms in biorthogonal labeling schemes on a monocyclooctynylated model protein ($GFP^{Y39\rightarrow BCN}$) and concluded that they can be useful tools for such purposes. We believe that these fluorogenic covalent cross-linking bistetrazine probes are ideal choices to directly visualize protein–protein interactions even by super-resolution microscopy. In comparison to bimolecular fluorescence complementation (BiFC) technology,[38] which is one of the most popular means to follow protein communications the presented bistetrazine probes in combination with Amber suppression technology are ideal surrogates. Unlike BiFC, where the original function is considerably perturbed by a comparable fusion tag and signal evolution is limited by the time required for assembly of the signaling fusion protein, the presented scaffolds require minimal perturbation in the structure of the protein studied and the fast kinetics of the inverse electron demand Diels-Alder reaction ensures real-time monitoring of protein–protein interactions. Work exploring these features is currently in progress in our laboratory and results will be reported in due course.

Experimental Section

General

All starting materials were obtained from commercial suppliers (Sigma-Aldrich, Merck, Alfa Aesar, Reanal, Molar Chemicals, Fluorochem) and used without further purification. Analytical thin-layer chromatography (TLC) was performed on silica gel 60 F254 precoated aluminum TLC plates from Merck. Column chromatography was carried out with silica gel (0.06–0.2 mm, Zeochem) or alumina (neutral, activated, Brockmann I, Sigma-Aldrich). Ratios of the solvents for the eluents are given in volumes (mL/mL). Microwave experiments were performed in an AntonPaar Monowave 400 microwave reactor. Semipreparative HPLC was performed on a Hanbon Semiprep NP7010C system using a Gemini C18 column (150 × 21 mm I.D.) with 5 µm silica (110 pore size) as a stationary phase. The samples were dissolved in DMSO. NMR spectra were recorded on a Varian Inova 500 MHz spectrometer. Chemical shifts (δ) are given in parts per million (ppm) using solvent signals as the reference for samples made in $CDCl_3$, or DMSO-d6. Analytical RP-HPLC-UV/Vis-MS experiments were performed on a SHIMADZU LCMS-2020 system using a Gemini C18 column (100 × 2.00 mm I.D.) with 5 µm silica (110 pore size) as a stationary phase with a photodiode array UV/Vis (220-800 nm) and an ESI-MS detector. Linear gradient elution (0 min 0% B; 1.0 min 100% B; 3.5 min 100% B; 4.5 min 0% B; 5.0 min 0% B) with eluent A (2% NH_4HCOO, 5% ACN and 93% water) and eluent B (2% NH_4HCOO 80% MeCN and 18% water) was used at a flow rate of 0.5 mL/min at 30°C. The samples were dissolved in the mixture of water and MeCN (1:1 V/V). The exact masses were determined with an Agilent 6230 time-of-flight mass spectrometer. All melting points were measured on an OptiMelt Automated Melting Point System and are uncorrected. The fluorescence and absorbance measurements were carried out on a Jasco FP8300 spectrofluorometer. Quartz cuvettes with path length of 1 cm were used.

Experimental Details

1-Ethyl-2-(3-(1-ethyl-5-iodo-3,3-dimethylindolin-2-ylidene)prop-1-en-1-yl)-5-iodo-3,3-dimethyl-3H-indol-1-ium iodide (**5**)

A mixture of 5-iodoindolium **4** (441 mg, 1.0 mmol) and triethyl othoformate (0.5 mL, 3.0 mmol) in pyridine (2.0 mL) were refluxed for 3 h. After cooling to r.t. the reaction mixture was poured into toluene and filtered. The solid was further washed with toluene. The solid was crystallized from EtOH to give **5** (337 mg, 88%) as shiny green crystals. R_f: 0.44 (CH_2Cl_2–MeOH 9:1). mp: 292–295°C decomp. (EtOH). ^{1}H NMR (500 MHz, DMSO-d6) δ 8.31 (t, *J* = 13.4 Hz, 1H), 8.04 (d, *J* = 1.6 Hz, 2H), 7.79 (dd, *J* = 8.3, 1.6 Hz, 2H), 7.31 (d, *J* = 8.4 Hz, 2H), 6.55 (d, *J* = 13.5 Hz, 2H), 4.14 (q, *J* = 7.1 Hz, 4H), 1.68 (s, 12H), 1.30 (t, *J* = 7.2 Hz, 6H). ^{13}C NMR (126 MHz, DMSO-d6) δ 172.9, 150.0, 149.5, 143.1, 141.3, 137.2, 131.2, 113.5, 102.8, 89.6, 48.9, 27.1, 12.1. HRMS $[M]^+$ calcd. for $[C_{27}H_{31}N_2I_2]^+$: 637.0577, found: 637.0601.

1-Ethyl-2-(3-(1-ethyl-3,3-dimethyl-5-(4-(6-methyl-1,2,4,5-tetrazin-3-yl)phenyl)indolin-2-ylidene)prop-1-en-1-yl)-3,3-dimethyl-5-(4-(6-methyl-1,2,4,5-tetrazin-3-yl)phenyl)-3H-indol-1-ium iodide (**6**)

A mixture of iodocyanine **5** (76.4 mg, 0.1 mmol), pinacol 4-(6-methyltetrazin-3-yl)phenylboronate (119 mg, 0.4 mmol, see supporting information), $Pd(dppf)Cl_2$ (14.6 mg, 0.02 mmol) and CsF (152 mg, 1.0 mmol) in acetonitrile (10 mL) were stirred at 80°C overnight. After cooling to r.t. the solvent was removed, and the residue was taken up in water and CH_2Cl_2. The aqueous layer was extracted 3 times with CH_2Cl_2, the combined organic phase was dried with $MgSO_4$, filtered through celite and the solvent was removed in vacuo. The crude product was purified with semipreparative HPLC using 1% HCOOH in water (A) – 1% HCOOH in MeOH (B) mixture as an eluent (0 min 5% B; 3 min 5% B; 25 min 100% B; 30 min 100% B; 32 min 0% B; 35 min 0% B) to give **6** (43 mg, 56%) as dark green shiny crystals. R_f: 0.36 (CH_2Cl_2–MeOH 9:1). mp: 176–179°C decomp. (water). ^{1}H NMR (500 MHz, DMSO-d6) δ 8.59 (d, *J* = 8.4 Hz, 4H), 8.42 (t, *J* = 13.4 Hz, 1H), 8.16 (d, *J* = 1.6 Hz, 2H), 8.08 (d, *J* = 8.5 Hz, 4H), 7.93 (dd, *J* = 8.2, 1.7 Hz, 2H), 7.63 (d, *J* = 8.5 Hz, 2H), 6.62 (d, *J* = 13.7 Hz, 2H), 4.25 (q, *J* = 7.0 Hz, 4H), 3.03 (s, 6H), 1.82 (s, 12H), 1.39 (t, *J* = 7.0 Hz, 6H). ^{13}C NMR (126 MHz, DMSO-d6) δ 173.5, 167.0, 163.0, 149.8, 143.1, 141.8, 141.7, 136.1, 130.7, 127.9, 127.8, 127.54, 127.52, 121.2, 111.9, 103.1, 49.1, 27.4, 20.8, 12.3. HRMS $[M]^+$ calcd. for $[C_{45}H_{45}N_{10}]^+$: 725.3829, found: 725.3860.

1-Ethyl-2-(3-(1-ethyl-3,3-dimethyl-5-(2-(6-methyl-1,2,4,5-tetrazin-3-yl)vinyl)indolin-2-ylidene)prop-1-en-1-yl)-3,3-dimethyl-5-(2-(6-methyl-1,2,4,5-tetrazin-3-yl)vinyl)-3H-indol-1-ium iodide (**7**)

In a microwave pressure tube a mixture of iodocyanine **5** (76.4 mg, 0.1 mmol), 2-(6-methyltetrazin-3-yl)ethyl methanesulfonate (131 mg, 0.6 mmol, see supporting information), Pd_2dba_3 (18.3 mg, 0.02 mmol), QPhos (14.2 mg, 0.02 mmol) and *N,N*-dicyclohexylmethylamine (214 mL, 1.0 mmol) in dry DMF (5 mL) were heated to 100°C and stirred for 60 min in a microwave reactor. The solvent was removed, the residue was first purified on alumina using CH_2Cl_2–MeOH (0 to 10% MeOH) as eluent, then with semipreparative HPLC using 1% HCOOH in water (A) – 1% HCOOH in MeOH (B) mixture as an eluent (0 min 5% B; 3 min 5% B; 25 min 100% B; 30 min 100% B; 32 min 0% B; 35 min 0% B) to give **7** (29 mg, 39%) as a dark purple solid. R_f: 0.33 (CH_2Cl_2–MeOH 9:1). mp: 139–142°C decomp. (water). ^{1}H NMR (500 MHz, DMSO-d6) δ 8.39 (t, *J* = 13.4 Hz, 1H), 8.31 – 8.27 (m, 4H), 7.92 (d, *J* = 8.4 Hz, 2H), 7.73 (d, *J* = 16.3 Hz, 2H), 7.56 (d, *J* = 8.3 Hz, 2H), 6.62 (d, *J* = 13.3 Hz, 2H), 4.21 (q, *J* = 6.7 Hz, 4H), 2.95 (s, 6H), 1.77 (s, 12H), 1.35 (t, *J* = 7.1 Hz, 6H). ^{13}C NMR (126 MHz, DMSO-

d6) δ 173.6, 166.0, 164.3, 151.4, 150.0, 142.9, 141.8, 139.1, 132.4, 130.3, 121.6, 120.5, 111.8, 103.7, 48.8, 27.4, 20.8, 12.3. HRMS $[M]^+$ calcd. for $[C_{37}H_{41}N_{10}]^+$: 625.3516, found: 625.3516.

Protein expression and labeling

Tagging experiment

We prepared a Maltose binding protein domain (MBP) construct, containing a FLAG-Tag as well as a short linker (KAEAADAEAAK) in front of the MBP sequence. The FLAG-tag and the linker were cloned by conventional overlap PCR and ligated into a pBAD-MBP-8His plasmid using restriction enzymes. In addition we also cloned variants, which harbored one or two Amber STOP codons instead of the lysine residues in the short linker sequence (KAEAADAEAA-Amber) and Amber-AEAADAEAA-Amber) by site directed mutagenesis. The short linker was designed in a way, so that in the case of incorporation of two cyclooctynylated noncanoncial amino acids (ncAAs) a cyclic product could be formed by reaction with a bis-tetrazine probe. The plasmids were co-transformed together with pEvol-PylRS^{AF} into Bl21(DE3) AI cells (Invitrogen). Expression was done in 500 ml TB medium adding 100 µg/ml Ampicillin (for the pBAD plasmid), 33 µg/ml Chloramphenicol (for the pEvol plasmid) and 0.5 ml of the corresponding overnight culture, shaking at 37°C. When the OD_{600} of 0.2 was reached, 1 mM of the SCO-lysine was added. The protein expression was induced with 0.02% Arabinose at an OD_{600} of 0.4-0.6. After 8-12 hours of incubation at 37°C, the cells were harvested by centrifugation. The pellets were taken up in 5 ml of lysis buffer (4×PBS, 0.2 mM TCEP, 1 mM PMSF, 5 mM imidazole) and sonicated on ice for 3× 30 seconds. After a one hour centrifugation step at 4°C at 20000 rpm, the cleared supernatant was incubated on nickel beads and washed with lysis buffer. After 1 hour, the nickel beads were collected in polypropylene columns and the protein was further purified with 10 mM imidazole in the lysis buffer and finally eluted with 500 mM imidazole in lysis buffer. To improve the purity of the protein, size exclusion chromatography was used. Protein concentration was estimated using a UV-spectrometer.

The labeling reaction was performed in a 0.2 ml PCR tube. 250 pmol of protein were mixed with 250 pmol of dye in a total 5 µl reaction (1xPBS, 0.2 mM TCEP) for 20 hours at RT. For each sample, 0.8 µl of the labeling reaction were mixed with 15 µl of 1×PBS and 5 µl 5×SDS loading dye, boiled for 5 minutes at 95°C and loaded on a NuPAGE 4-12% SDS-PAGE (Invitrogen). After gel electrophoresis in MOPS buffer, the SDS-PAGE was scanned on a fluorescence scanner at 532 nm. The emission signal was collected from 570 nm on. Finally the gel was stained with Coomassie blue.

Crosslinking experiment

The previously reported construct, pBAD-GFP$^{Y39\rightarrow TAG}$ was co-transformed with the pEvol-PylRS^{AF} plasmid into Bl21 (DE3) AI cells.[7b] Expression was done in 500 ml TB at 37°C in a shaker. At OD_{600} of 0.2, 1 mM of BCN-lysine was added to the medium. 0.02% Arabinose was used to induce the protein expression at OD_{600}=0.4. The culture was incubated for 8-12 hours at 37°C and harvested by centrifugation. The same purification protocol was followed as described above for the MBP constructs.

For the labeling reaction 50 pmol of GFP$^{Y39\rightarrow BCN}$ were mixed with 50 pmol of dye in a 10 µl reaction using 1×PBS to fill up the reaction mix. For each time point, 1µl of the labeling reaction was mixed with 8 µl 1×PBS and 1 µl 10 mM BCN-Lysine, to stop the labeling reaction immediately. Each sample was mixed with 5×SDS-loading dye and boiled at 95°C before loading on a NuPAGE 4-12% SDS-PAGE. Gel electrophoresis was carried out using MOPS buffer. The SDS-PAGE gels were scanned on a fluorescent scanner at 532 nm and stained with Coomassie blue.

Acknowledgements

Present work was supported by the Hungarian Scientific Research Fund (OTKA, NN-116265) and the "Lendület" Program of the Hungarian Academy of Sciences (LP2013-55/2013). EAL acknowledges funding from the SPP1623. The authors thank the Proteomics core facility (EMBL Heidelberg) for technical support.

Keywords: bioorthogonal • fluorogenic probes • non-canonical amino acid • two-point labeling • fluorogenic crosslinker

[1] C. Freidel, S. Kaloyanova, K. Peneva, *Amino Acids.* **2016**, *48*, 1357–1372.
[2] Y. Gong, L. Pan, *Tetrahedron Lett.* **2015**, *56*, 2123–2132.
[3] G. Zhang, S. Zheng, H. Liu, P. R. Chen, *Chem. Soc. Rev.* **2015**, *44*, 3405–3417.
[4] J. Lotze, U. Reinhardt, O. Seitz, A. G. Beck-Sickinger, *Mol. BioSyst.* **2016**, *12*, 1731–1745.
[5] C. Li, A. G. Tebo, A. Gautier, *Int. J. Mol. Sci*. **2017**, *18*, 1473–1483.
[6] E. Kozma, O. Demeter, P. Kele, *ChemBioChem* **2017**, *18*, 486–501.
[7] a) T. Plass, S. Milles, C. Koehler, J. Szymański, R. Mueller, M. Wießler, C. Schultz, E. A. Lemke, *Angew. Chem. Int. Ed*. **2012**, *51*, 4166–4170; b) T. Plass, S. Milles, C. Koehler, C. Schultz, E. Lemke, *Angew. Chem. Int. Ed* **2011**,*50*, 3878–3881.
[8] I. Nikić, T. Plass, O. Schraidt, J. Szymański, J. A. Briggs, C. Schultz, E. A. Lemke, *Angew. Chem. Int. Ed.* **2014**, *53*, 2245–2249.
[9] E. Kozma, I. Nikić, B. R. Varga, I. V. Aramburu, J. H. Kang, O. T. Fackler, E. A. Lemke, P. Kele, *ChemBioChem* **2016**, *17*, 1518–1524.
[10] J.-E. Hoffmann, T. Plass, I. Nikić, I. V. Aramburu, C. Koehler, H. Gillandt, [8] E. A. Lemke, C. Schultz, *Chem. Eur. J.* **2015**, *21*, 12266–12270.
[11] G. B. Cserép, A. Herner, P. Kele, Methods *Appl. Fluoresc*. **2015**, *3*, 042001.
[12] A. Nadler, C. Schultz, *Angew. Chem. Int. Ed.* **2013**, *52*, 2408–2410.
[13] a) P. Shieh, V. T. Dien, B. J. Beahm, J. M. Castellano, T. Wyss-Coray, C. R. Bertozzi, *J. Am. Chem. Soc.* **2015**, *137*, 7145–7151; b) N. K. Devaraj, S. Hilderbrand, R. Upadhyay, R. Mazitschek, R. Weissleder, Angew. Chem. Int. Ed. **2010**, *49*, 2869–2872.
[14] a) A. Herner, G. Estrada Girona, I. Nikić, M. Kállay, E. A. Lemke, P. Kele, *Bioconjugate Chem.* **2014**, *25*, 1370–1374; b) A. Herner, I. Nikić, M. Kállay, E. A. Lemke, P. Kele, *Org. Biomol. Chem.*, **2013**, *11*, 3297–3306.
[15] a) A. Wieczorek, P. Werther, J. Euchner, R. Wombacher, *Chem. Sci.* **2017**, *8*, 1506–1510; b) L. G. Meimetis, J. C. T. Carlson, R. J. Giedt, R. H. Kohler R. Weissleder, *Angew. Chem. Int. Ed.* **2014**, *53*, 7531–7534; c) J. C. T. Carlson, L. G. Meimetis, S. A. Hilderbrand, R. Weissleder, *Angew. Chem. Int. Ed.* **2013**, *52*, 6917–6920.
[16] K. Lang, L. Davis, S. Wallace, M. Mahesh, D. J. Cox, M. L. Blackman, J. M. Fox, J. W. Chin, *J. Am. Chem. Soc.* **2012**, *134*, 10317–10320.
[17] Y. Chen, K. Tsao, J. W. Keillor, *Can. J. Chem.* **2015**, *93*, 389–398.
[18] S. R. Adams, R. Y. Tsien, *Nat. Prot*oc. **2008**, *3*, 1527–1534.
[19] a) S. Girouard, M.-H. Houle, A. Grandbois, J. Keillor, S. Michnick, *J. Am. Chem. Soc.* **2005**,*127*, 559–566; b) J. Guy, K. Caron, S. Dufresne, S. Michnick, Skene, J. Keillor, *J. Am. Chem. Soc.* **2007**, *129*, 11969–11977.
[20] a) O. Demeter, E. A. Fodor, M. Kállay, G. Mező, K. Németh, P. T. Szabó, P. Kele, *Chem. Eur. J.* **2016**, *22*, 6382–6388; b) O. Demeter, A. Kormos, C. Koehler, G. Mező, K. Németh, E. Kozma, L. B. Takacs, E. A. Lemke, P. Kele, *Bioconjugate Chem.* **2017**, *28*, 1552–1559.
[21] a) J. C. Anderson, P. G. Schultz, *Biochemistry* **2003**, *42*, 9598–9608; b) S. Milles, S. Tyagi, N. Banterle, C. Koehler, V. VanDelinder, T. Plass, A. Neal, E. Lemke, *J. Am. Chem. Soc.* **2012**, *134*, 5187–5195.
[22] J. C. Anderson, N. Wu, S. W. Santoro, V. Lakshman, D. S. King, P. G. Schultz, *Proc. Natl. Acad. Sci. U.S.A.* **2004**, *101*, 7566–7571.

[23] M. Amiram, A. D. Haimovich, C. Fan, Y.-S. Wang, H.-R. Aerni, I. Ntai, D. W. Moonan, N. J. Ma, A. J. Rovner, S. H. Hong, N. L. Kelleher, A. L. Goodman, M. C. Jewett, D. Söll, J. Rinehart, F. J. Isaacs, *Nat. Biotechnol.* **2015**, *33*, 1272–1279.

[24] G. L'abbe, *Chem. Rev*. **1969**, *69*, 345–363.

[25] M. Levitus, S. Ranjit, *Q. Rev. Biophys.* **2011**, *44*, 123–151.

[26] K. Klehs, C. Spahn, U. Endesfelder, S. F. Lee, A. Fürstenberg, M. Heilemann, *ChemPhysChem*, **2014**, *15*, 637–641.

[27] A. Borrmann, S. Milles, T. Plass, J. Dommerholt, J. M. M. Verkade, M. Wiessler, C. Schultz, J. C. M. van Hest, F. L. van Delft, E. A. Lemke, *ChemBioChem*, **2012**, *13*, 2094–2099.

[28] E. Neuteboom, S. Meskers, E. Beckers, S. Chopin, R. Janssen, *J Phys Chem* **2006**, *110*, 12363–12371.

[29] a) J. Guy, R. Castonguay, N. Pineda, V. Jacquier, K. Caron, S. Michnick, J. Keillor,*Mol. Biosyst.* **2010**, *6*, 976–987; b) Y. Chen, C. M. Clouthier, K. Tsao, M. Strmiskova, H. Lachance, J. W. Keillor, *Angew. Chem. Int. Ed. Engl.* **2014**, *53*, 13785–13788; c) X. Pan , Z. Liang, J. Li, S. Wang, F. Kong, K. Xu, B. Tang, *Chem. Eur. J.* **2015**,*21*, 2117–2122.

[30] H. Cao, Y. Xiong, T. Wang, B. Chen, T. C. Squier, M. U. Mayer, *J. Am. Chem. Soc.* **2007**, *129,* 8672–8673.

[31] S. C. Alexander, A. Schepartz, *Org. Lett.* **2014**, *16*, 3824–3827.

[32] A. Pomorski, A. Krężel, *ChemBioChem* **2011**, *12*, 1152–1167.

[33] N. Fu, Y. Xiong, T. C. Squier, *J. Am. Chem. Soc.* **2012**, *134*, 18530–18533.

[34] N. W. Luedtke, R. J. Dexter, D. B. Fried, A. Schepartz, *Nat. Chem. Biol.* **2007**, *3*, 779–784.

[35] J. L. Goodman, D. B. Fried, A. Schepartz, *ChemBioChem* **2009**, *10*, 1644-1647.

[36] A. Rutkowska, C. H. Haering, C. Schultz, *Angew. Chem. Int. Ed*. **2011**, *50*, 12655–12658.

[37] T. L. Halo, J. Appelbaum, E. M. Hobert, D. M. Balkin, A. Schepartz, *J. Am. Chem. Soc*. **2009**, *131*, 438–439.

[38] S. Xing, N. Wallmeroth, K. W. Berendzen, C. Grefen, *Plant Physiol.* **2016**, *171*, 727–758.

10.1002/chem.201800910

WILEY-VCH

Entry for the Table of Contents

FULL PAPER

The synthesis, fluorogenic and conjugation characteristics of two new bistetrazine-cyanine probes are presented. The probes can bind to genetically altered proteins harboring an 11-amino acid peptide tag with two appending cyclooctyne motifs. Fluorogenic cross-linking potential of the probes is also presented with monocyclooctynylated proteins.

Attila Kormos, Christine Koehler, Eszter A. Fodor, Zsófia R. Rutkai, Madison E. Martin, Gábor Mező, Edward A. Lemke, and Péter Kele**

Page No. – Page No.

Bistetrazine-cyanines as double-clicking fluorogenic two-point binder or crosslinker probes